

Fig. 4. XRD patterns of the synthesized nanocomposite ($\text{Mn}(\text{BH}_4)_2 + 2\text{LiCl}$) after dehydrogenation at 100°C for 18.7 h.

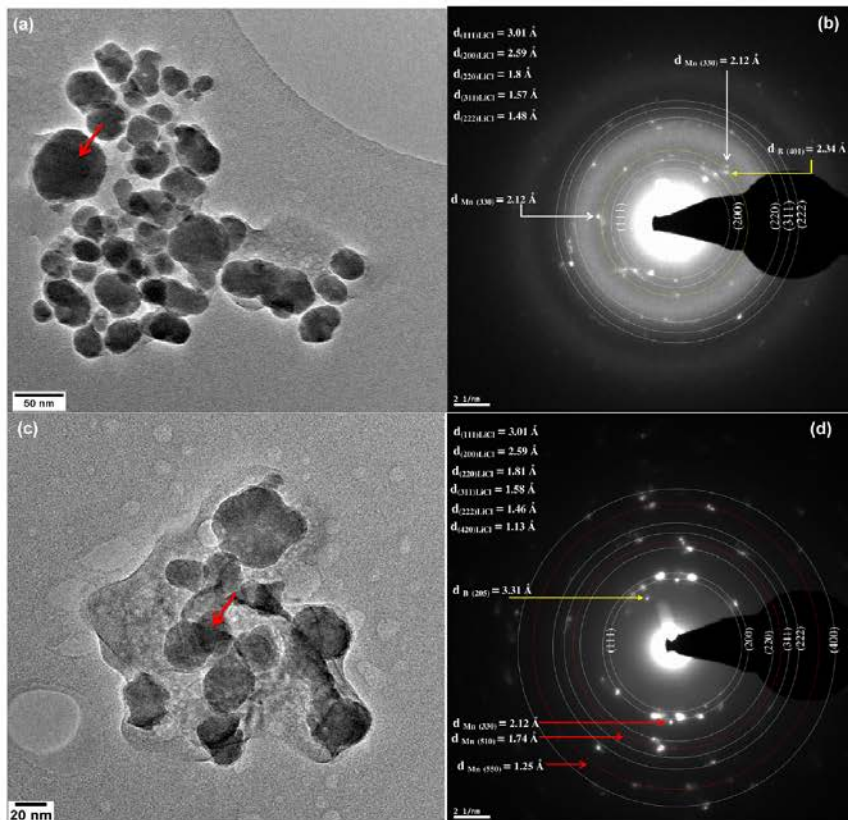
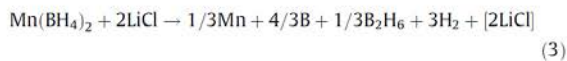


Fig. 5. (a and c) TEM micrograph of the synthesized nanocomposite ($\text{Mn}(\text{BH}_4)_2 + 2\text{LiCl}$) (dry condition) after dehydrogenation at 100°C (18.7 h) and (b and d) corresponding selected SAED patterns.



The theoretical capacity of reaction (3) is 3.58 wt.% H_2 and 9.0 wt.% for a gas mixture ($3\text{H}_2 + 1/3\text{B}_2\text{H}_6$). In reactions (2) and

(3) both Mn and B are being formed so the microstructural phase composition of samples after reactions (2) and (3) is the same.

The XRD pattern for the synthesized nanocomposite ($\text{Mn}(\text{BH}_4)_2 + 2\text{LiCl}$) after dehydrogenation at 100°C for 18.7 h is presented in Fig. 4 and after dehydrogenation at 150 and 200°C

Table 2
Interplanar spacings and Bragg diffraction angles 2θ for α -Mn as compared to experimentally observed TEM SAED patterns.

α -Mn ICDD (JCPDC) card #32-0637		(SAEDP) this work
$d_{(hkl)}$ (Å)	I [%]	$d_{(hkl)}$ (Å)
2.10110	100.0	2.12
1.89900	25.0	–
1.81900	9.0	–
1.74750	14.0	1.74
1.28640	4.0	–
1.26050	7.0	1.25

in Fig. 4S (Supplement). Comparing it with Fig. 1 (just after MCAS) it can be seen that no peaks of $\text{Mn}(\text{BH}_4)_2$ are visible anymore while the LiCl peaks remains very strong. It is to be noted that no X-ray diffraction peaks of pure elemental Mn and B are visible in Figs. 4 and 4S as would be theoretically expected due to the proposed paths of thermal decomposition in both reactions (2) and (3).

Fig. 5a and c show the TEM micrographs for the same synthesized nanocomposite ($\text{Mn}(\text{BH}_4)_2 + 2\text{LiCl}$) after thermal dehydrogenation at 100 °C for 18.7 h whose XRD pattern is already shown in Fig. 4. Nearly round-shaped nanoscale particles are clearly visible in a larger agglomeration. The corresponding SAED patterns from the areas indicated by the red arrows in Fig. 5a and c are shown in Fig. 5b and d, respectively. Electron diffraction spots corresponding to the lattice planes of LiCl such as (111), (200), (220), (311) and (222), identified using ICDD (JCPDC) card #74-1972, are clearly observed distributed on the calculated diffraction rings corresponding to randomly oriented nanoparticles in Fig. 5a and c.

However, the most interesting finding is that a number of electron diffraction spots corresponding to crystalline α -Mn (space group I3m) and β -B rhombohedral (space group R3m) are also identified using ICDD (JCPDC) card #32-0637 and #11-0618,

respectively. The most intense diffracting planes for α -Mn are collected in Table 2 including the lattice spacings ($d_{(hkl)}$) and peak intensities. According to Table 2 the strongest peak (100%) of α -Mn is assigned to the (330) plane with the $d_{(330)}$ spacing of 2.10 Å. The SAED patterns of annealed powder in Fig. 5b and d show strong diffraction spots of α -Mn corresponding to the diffraction planes (330), (510) and (550) (Table 2) distributed on the calculated diffraction rings which were calculated by the ImageJ software [20] based on the scale of the corresponding SAED pattern.

The first three strongest diffraction peaks of β -B occur at small diffraction angles of $2\theta = 11.12, 17.51$ and 19.02° and conversely at larger $d_{(hkl)}$ spacings whose corresponding electron diffraction spots would be located very close to the center of SADPs in Fig. 5b and d. Unfortunately, they cannot be discerned in the respective SAED patterns because of the presence of a background coming from the fact that the particles are very small and distributed over an amorphous carbon film in Fig. 5b and d. Nevertheless, two electron diffraction spots from the lattice planes (205) and (401) with the lattice spacing $d_{(401)} = 2.34$ Å and $d_{(205)} = 3.31$ Å, belonging to β -B, are clearly detected in the SAED patterns in Fig. 5b and d.

The evidence that both Mn and B exist in the dehydrogenated powder as the crystalline phases α -Mn and β -B, respectively, is another important finding in this work. It was shown earlier that the XRD pattern of the dehydrogenated ($\text{Mn}(\text{BH}_4)_2 + 2\text{LiCl}$) nanocomposite shown in Fig. 4 does not show any visible Bragg diffraction peaks belonging to crystalline Mn or B. In the cases where no crystalline diffraction peaks are present it is often assumed “a priori” that the decomposition products of $\text{Mn}(\text{BH}_4)_2$ are amorphous [11,12,15]. However, to the contrary, the SAED patterns clearly show that both Mn and B products exit after dehydrogenation of $\text{Mn}(\text{BH}_4)_2$ in a crystalline form. For the sake of clarity, it is to be noted that in [10] we observed very small but recognizable diffraction peaks of α -Mn after dehydrogenation of the synthesized mixtures ($n\text{LiBH}_4 + \text{MnCl}_2$) where $n = 5, 9$ and 23. No XRD peaks corresponding to crystalline α -Mn have ever been observed for

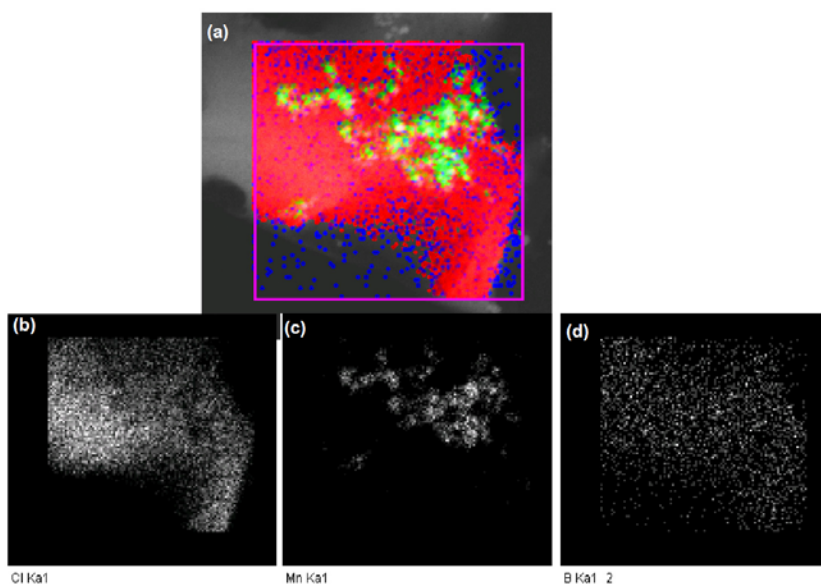


Fig. 6. (a) The energy X-ray dispersive spectroscopy (EDS) elemental distribution map after dehydrogenation at 100 °C (18.7 h) and decomposition of $\text{Mn}(\text{BH}_4)_2$ for all elements: Cl (red), Mn (green) and B (blue). Individual elemental distribution maps for (b) Cl, (c) Mn and (d) B. (For interpretation of the references to colour in this figure legend, the reader is referred to the web version of this article.)

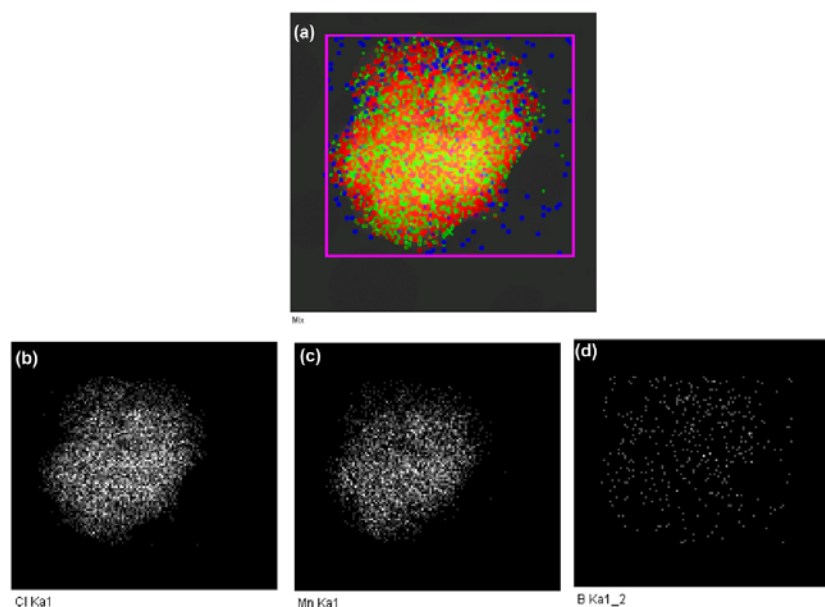


Fig. 7. (a) The energy dispersive X-ray spectroscopy (EDS) elemental distribution map for the synthesized nanocomposite ($\text{Mn}(\text{BH}_4)_2 + 2\text{LiCl}$) after ball milling with an energy input $Q_{\text{TR}} = 145.6 \text{ kJ/g}$ (2 h) for all elements: Cl (red), Mn (green) and B (blue). Individual elemental distribution maps for (b) Cl, (c) Mn and (d) B. (For interpretation of the references to colour in this figure legend, the reader is referred to the web version of this article.)

the molar ratio $n = 2$. Neither XRD peaks of crystalline β -B have ever been observed after dehydrogenation of $\text{Mn}(\text{BH}_4)_2$ for any molar ratio n in the ($n\text{LiBH}_4 + \text{MnCl}_2$) mixture [2,3,6–12,15].

In general, it must be pointed out that from reactions (2) and (3) the quantity of LiCl after desorption is 2 mol in the total mass of powder which is much larger than only 1 mol of Mn or B. Therefore, LiCl will be well detectable by XRD in contrast to Mn/B whose quantity could be insufficient to be detectable by XRD although Mn/B are detectable by electron diffraction which is capable of analyzing very small powder particles. The SAEDPs in Fig. 5a and c were taken from powder particles (red arrows) having sizes on the order of 20–50 nm. Since the SAEDPs show diffraction spots of LiCl, α -Mn and β -B, all these phases must have nanometric sizes to be confined within the 20–50 nm sized particles. Additional support for the presence of nanometric-size α -Mn and β -B after thermal dehydrogenation of the ($\text{Mn}(\text{BH}_4)_2 + \text{MnCl}_2$) nanocomposite and decomposition of $\text{Mn}(\text{BH}_4)_2$ is provided by the EDS elemental distribution map for all elements: Cl (red), Mn (green) and B (blue) in Fig. 6a and particularly by the individual elemental maps for Cl (Fig. 6b), Mn (Fig. 6c) and B (Fig. 6d) from the powder thermally dehydrogenated at 100 °C for 18.7 h whose XRD pattern is already shown in Fig. 4 and HR TEM images and SAED patterns are shown in Fig. 5. For comparison to Fig. 6 the same EDS elemental distribution maps were taken from a synthesized nanocomposite ($\text{Mn}(\text{BH}_4)_2 + \text{MnCl}_2$) after ball milling and are shown in Fig. 7. It is clearly seen, especially from individual EDS elemental maps that both the $\text{MnK}_{\alpha 1}$ (Fig. 7c) and $\text{BK}_{\alpha 1}$ (Fig. 7d) elements are very uniformly dispersed in the ball milled powder containing the synthesized $\text{Mn}(\text{BH}_4)_2$ phase while after thermal decomposition of $\text{Mn}(\text{BH}_4)_2$ the Mn element, as can be seen in its $\text{MnK}_{\alpha 1}$ elemental map (Fig. 6c), is agglomerated into clusters, most likely, forming the α -Mn nanograins. There is no such a pronounced clustering observed in the elemental $\text{BK}_{\alpha 1}$ map (Fig. 6d) for dispersion of β -B after decomposition of $\text{Mn}(\text{BH}_4)_2$ as compared to its dispersion after ball milling in the elemental $\text{BK}_{\alpha 1}$ map in Fig. 7d.

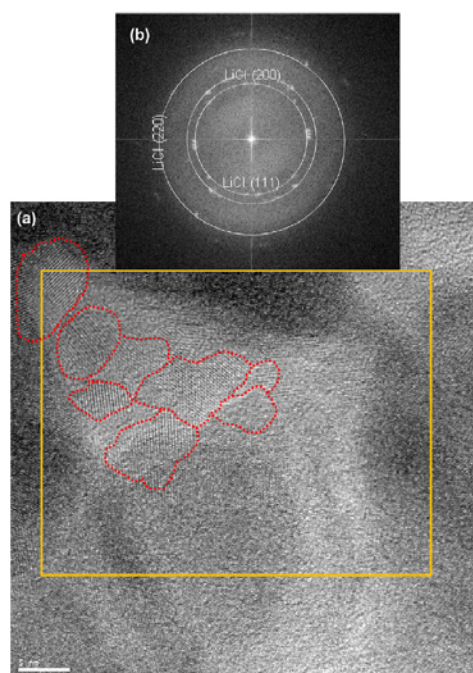


Fig. 8. (a) High resolution TEM micrograph of the initial synthesized nanocomposite ($\text{Mn}(\text{BH}_4)_2 + 2\text{LiCl}$) after thermal dehydrogenation at 100 °C for 18.7 h. (b) A digital SAEDP using a fast Fourier transform (FFT) of the area inside the box in (a) (marker 5 nm).

A high resolution TEM image of the synthesized nanocomposite after thermal dehydrogenation (Figs. 4 and 5) is shown in Fig. 8a which was taken from one of the powder particles visible in Fig. 5c. Nanograins with different crystal orientations, which are contoured by a red broken line, can be clearly seen. Employing FFT from the rectangle area indicated in Fig. 8a identifies those nanograins as belonging to LiCl. The digital diffraction patterns obtained using FFT in Fig. 8b presents two calculated electron diffraction rings which exactly conform to the diffraction pattern of the fcc structure of LiCl. The average ECD for the LiCl nanograins visible in Fig. 8a was estimated as being equal to 6.1 ± 1.8 nm. This value correlates well with the nanograin size of the LiCl phase after MCAS synthesis observed in the ball milled powder particles (Fig. 3).

4. Summary and conclusions

Mechano-chemical activation synthesis (MCAS) using a magneto ball mill was employed to synthesize the nanocomposite ($\text{Mn}(\text{BH}_4)_2 + 2\text{LiCl}$) from the initial ($2\text{LiBH}_4 + \text{MnCl}_2$) powder mixture. Ball milling was carried out under the milling energy input $Q_{\text{TR}} = 145.6$ kJ/g. Both X-ray diffraction and TEM selected area electron diffraction patterns (SAEDPs) clearly confirm the presence of the $\text{Mn}(\text{BH}_4)_2$ and LiCl phases in the synthesized nanocomposite. No other phases were detected. Both $\text{Mn}(\text{BH}_4)_2$ and LiCl are nanocrystalline phases because bright field high-resolution TEM imaging of the synthesized composite powder particles reveals the presence of nanograins belonging to LiCl and $\text{Mn}(\text{BH}_4)_2$. The grain sizes expressed as the equivalent circle diameters (ECD) of LiCl and $\text{Mn}(\text{BH}_4)_2$, estimated from the high-resolution TEM micrographs, are within the range of 14.1 ± 3.7 nm and 10.0 ± 2.9 nm, respectively.

The XRD patterns of the thermally dehydrogenated ($\text{Mn}(\text{BH}_4)_2 + 2\text{LiCl}$) nanocomposite do not exhibit any visible Bragg diffraction peaks belonging to either crystalline α -Mn or β -B. In contrast, the SAED patterns and EDS elemental maps provide convincing evidence that both Mn and B exist in the dehydrogenated powder as the nanometric-size phases α -Mn and β -B, respectively. Apparently, the lack of Bragg diffraction peaks in an XRD pattern is insufficient evidence that the Mn and B elemental products of $\text{Mn}(\text{BH}_4)_2$ thermal dehydrogenation can be classified as being amorphous.

Acknowledgments

This research was supported by the NSERC Discovery and NSERC Hydrogen Canada (H2CAN) Strategic Research Network Grants which are gratefully acknowledged.

Appendix A. Supplementary data

Supplementary data associated with this article can be found, in the online version, at <http://dx.doi.org/10.1016/j.actamat.2015.08.038>.

References

- [1] D.S. Scott, Smelling Land – the Hydrogen Defense Against Climate Catastrophe, Canadian Hydrogen Association, Westmount, QC, 2007.
- [2] R.A. Varin, T. Czujko, Z.S. Wronski, Nanomaterials for Solid State Hydrogen Storage, Springer Science + Business Media, New York, 2009.
- [3] R.A. Varin, Z.S. Wronski, Progress in hydrogen storage in complex hydrides, Ch. 13, in: L.M. Gandia, G. Arzamendi, P.M. Diéguez (Eds.), Renewable Hydrogen Technologies. Production, Purification, Storage, Applications and Safety, Elsevier, 2013, pp. 293–332. ISBN: 978-0-444-56352-1.
- [4] J. Yang, A. Sudik, C. Wolverton, D.J. Siegel, High capacity hydrogen storage materials: attributes for automotive applications and techniques for materials discovery, Chem. Soc. Rev. 39 (2010) 656–675.
- [5] <http://energy.gov/sites/prod/files/2014/03/12/targets_onboard_hydro_storage.pdf>.
- [6] R.A. Varin, A.R. Shirani Bidabadi, Nanostructured complex hydride systems for hydrogen generation, AIMS Energy 3 (2015) 121–143.
- [7] R. Černý, N. Penin, H. Hagemann, Y. Filinchuk, The first crystallographic and spectroscopic characterization of a 3d-metal borohydride: $\text{Mn}(\text{BH}_4)_2$, J. Phys. Chem. C 113 (2009) 9003–9007.
- [8] P. Choudhury, S.S. Srinivasan, V.R. Bhethanabotla, Y. Goswami, K. McGrath, E.K. Stefanakos, Nano-Ni doped Li–Mn–B–H system as a new hydrogen storage candidate, Int. J. Hydrogen Energy 34 (2009) 6325–6334.
- [9] R.A. Varin, L. Zbronec, The effects of ball milling and nanometric nickel additive on the hydrogen desorption from lithium borohydride and manganese chloride ($3\text{LiBH}_4 + \text{MnCl}_2$) mixture, Int. J. Hydrogen Energy 35 (2010) 3588–3597.
- [10] R.A. Varin, L. Zbronec, M. Polanski, Y. Filinchuk, R. Černý, Mechano-chemical synthesis of manganese borohydride ($\text{Mn}(\text{BH}_4)_2$) and inverse cubic spinel (Li_2MnCl_4) in the ($n\text{LiBH}_4 + \text{MnCl}_2$) ($n = 1, 2, 3, 5, 9$ and 23) mixtures and their dehydrogenation behavior, Int. J. Hydrogen Energy 37 (2012) 16056–16069.
- [11] R. Liu, D. Reed, D. Book, Decomposition behaviour of $\text{Mn}(\text{BH}_4)_2$ formed by ball-milling LiBH_4 and MnCl_2 , J. Alloys Compd. 515 (2012) 32–38.
- [12] R.A. Varin, A.R. Shirani Bidabadi, The effect of milling energy input during mechano-chemical activation synthesis (MCAS) of the nanocrystalline manganese borohydride ($\text{Mn}(\text{BH}_4)_2$) on its thermal dehydrogenation properties, Int. J. Hydrogen Energy 39 (2014) 11620–11632.
- [13] R.A. Varin, A.R. Shirani Bidabadi, Rapid, ambient temperature hydrogen generation from the solid state Li–B–Fe–H system by mechano-chemical activation synthesis, J. Power Sources 284 (2015) 554–565.
- [14] G. Severa, H. Hagemann, M. Longhini, J.W. Kaminski, T.A. Wesolowski, C.M. Jansen, Thermal desorption, vibrational spectroscopic, and DFT computational studies of the complex manganese borohydrides $\text{Mn}(\text{BH}_4)_2$ and $[\text{Mn}(\text{BH}_4)_4]^{2-}$, J. Phys. Chem. C 114 (2010) 15516–15521.
- [15] B. Richter, D.B. Ravnsbaek, N. Tumanov, Y. Filinchuk, T.R. Jensen, Manganese borohydride: synthesis and characterization, Dalton Trans. (2015).
- [16] A. Calka, A.P. Radlinski, Universal high performance ball-milling device and its application for mechanical alloying, Mater. Sci. Eng., A 134 (1991) 1350–1353.
- [17] Patents: WO9104810, US5383615, CA2066740, EP0494899, AU643949.
- [18] A. Calka, R.A. Varin, Application of controlled ball milling in materials processing, in: T.S. Srivatsan, R.A. Varin, M. Khor (Eds.), Int. Symp. on Processing and Fabrication of Advanced Materials IX (PFAM IX), ASM International, Materials Park, OH, 2001, pp. 263–287.
- [19] M. Mamatha, B. Bogdanović, M. Felderhoff, A. Pommerin, W. Schmidt, F. Schüth, C. Weidenthaler, Mechanochemical preparation and investigation of properties of magnesium, calcium and lithium–magnesium alanates, J. Alloys Compd. 407 (2006) 78–86.
- [20] <<http://imagej.en.softonic.com/>>.
- [21] R. Parviz, R.A. Varin, Combined effects of molar ratio and ball milling energy on the phase transformations and mechanical dehydrogenation in the lithium amide–magnesium hydride ($\text{LiNH}_2 + n\text{MgH}_2$) ($n = 0.5–2$) nanocomposites, Int. J. Hydrogen Energy 38 (2013) 8313–8327.
- [22] J.-Ph. Soulie, G. Renaudin, R. Cerny, K. Yvon, Lithium borohydride LiBH_4 . Crystal structure, J. Alloys Compd. 346 (2002) 200–205.
- [23] H.E. Swanson, H.F. McMurdie, M.C. Morris, E.H. Evans, X-ray powder diffraction powder patterns, Natl. Bur. Stand. Monogr. 25 (Section 8) (1970) 1–171.
- [24] R. Cerny, N. Penin, V. Danna, H. Hagemann, E. Durand, J. Ruzicka, $\text{Mg}_x\text{Mn}_{1-x}(\text{BH}_4)_2$ ($x = 0–0.8$), a cation solid solution in a bimetallic borohydride, Acta Mater. 59 (2011) 5171–5180.
- [25] C.E. Krill, R. Birringer, Estimating grain-size distributions in nanocrystalline materials from X-ray diffraction profile analysis, Philos. Mag. A 77 (1998) 621–640.
- [26] Z. Zhang, F. Zhou, E.J. Lavernia, On the analysis of grain size in bulk nanocrystalline materials via X-Ray diffraction, Metall. Mater. Trans. A 34A (2003) 1349–1355.
- [27] T. Ungár, The meaning of size obtained from broadened diffraction peaks, Adv. Eng. Mater. 5 (2003) 323–329.

4.7. Weight percent of a hydride phase and hydrogen by DSC method

In DSC measurements, the weight percent of a phase can be calculated using the peak area of the DSC curve and its reported heat of formation (enthalpy of formation) if it is available. For example, weight percent of the β -MgH₂ in a reactively milled powder can be estimated using the peak area of the DSC curves and the reported β -MgH₂ heat of formation (-74 kJ/mol [116], which equals to -2811 J/g). The DSC curve was analyzed by the NETZSCH thermal analysis software. First, the onset and end temperature of the peak were determined. Then, the peak area was calculated using the linear approach from the onset temperature to the end temperature (Fig. 4.14) by the DSC software.

The weight percent of β -MgH₂ is given by:

$$\text{wt\% of } \beta\text{-MgH}_2 = \text{peak area (J/g)} / \beta\text{-MgH}_2 \text{ heat of decomposition (J/g)}$$

where heat of decomposition = -(heat of formation)

From the decomposition of β -MgH₂ ($\text{MgH}_2 \rightarrow \text{Mg} + \text{H}_2$), the weight percent of desorbed hydrogen can be calculated by:

$$\text{wt.\% of H}_2 = \text{wt.\% of MgH}_2 \times (\text{molecular weight of H}_2 / \text{molecular weight of MgH}_2)$$

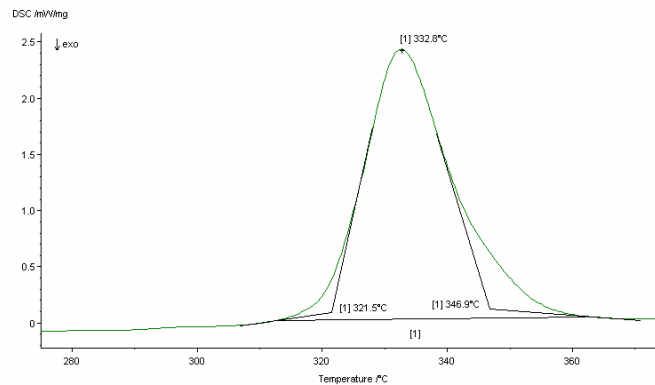


Fig. 4.14. Schematic of calculating the weight percent of a hydride phase by DSC analysis [10].

References

[1] Hubbert peak theory. https://en.wikipedia.org/wiki/Hubbert_peak_theory.

[2] M.K. Hubbert. https://en.wikipedia.org/wiki/M._King_Hubbert.

- [3] J.O.M. Bockris. *Int. J. Hydrogen Ener.* 32 (2007) 153-158.
- [4] G. Wrightstone. *INCONVENIENT FACTS: The science that Al Gore doesn't want you to know* (Kindle Locations 280-282). Mill City Press. Kindle Edition, 2017.
- [5] K. Hashimoto, H. Habazaki, M. Yamasaki, S. Meguro, T. Sasaki, H. Katagiri, T. Matsui, K. Fujimura, K. Izumiya, N. Kumagai, E. Akiyama. *Mater. Sci. Eng. A* 304-306 (2001) 88-96.
- [6] B. Yildiz, M.S. Kazimi. *Int. J. Hydrogen Ener.* 31(2006) 77-92.
- [7] J.A. Turner, M.C. Williams, K. Rajeshwar, *The Electrochem. Soc. Interface* 13(3) (2004) 24-30.
- [8] B.C.R. Ewan, R.W.K. Allen, "A figure of merit assessment of the routes to hydrogen", *Int. J. Hydrogen Energy* 30 (2007) 809-819.
- [9] 2018 Cost Projections of PEM Fuel Cell Systems for Automobiles and Medium-Duty Vehicles. <https://www.energy.gov/eere/fuelcells/downloads/2018-cost-projections-pem-fuel-cell-systems-automobiles-and-medium-duty>.
- [10] R.A. Varin, T. Czujko, Z.S. Wronski, "Nanomaterials for Solid State Hydrogen Storage", Springer Science+Business Media, LLC 2009, New York, USA, 2009 (ISBN: 978-0-387-77711-5; e-ISBN: 978-0-387-77712-2).
- [11] A. Abbaspour, N. Parsa, M. Sadeghi. *Int. J. Computer Applications* 97 (2014) 25-32
- [12] What is a Fuel Cell? <http://www.fuelcellstore.com/blog-section/what-is-a-fuel-cell>
- [13] Proton exchange membrane fuel cell. https://en.wikipedia.org/wiki/Proton-exchange_membrane
- [14] V. Ramani, H.R. Kunz, J.M. Fenton, "The polymer electrolyte fuel cell", *The Electrochem. Soc. Interface* 13(3) (2004) 17-45.
- [15] Toyota Mirai fuel cell stack SAO 2016. https://commons.wikimedia.org/wiki/File:Toyota_Mirai_fuel_cell_stack_SAO_2016_9034.jpg.
- [16] 2017 Mirai Product Information. <https://ssl.toyota.com/mirai/assets/core/Docs/Mirai%20Specs.pdf>
- [17] Toyota Mirai Technical Specifications. media.toyota.co.uk/wp.../files.../1444919532151015MToyotaMiraiTechSpecFinal.pdf
- [18] Target Explanation Document: Onboard Hydrogen Storage for Light-Duty Fuel Cell Vehicles 2017. https://energy.gov/sites/prod/files/2017/05/f34/fcto_targets_onboard_hydro_storage_explanation.pdf.
- [19] G. Sandi. *The Electrochem. Soc. Interface* 13(3) (2004) 40-44.

- [20] 2018 Mirai.
https://ssl.toyota.com/mirai/assets/.../Docs/MY18_Mirai_eBrochure_FuelCellTech.pdf
- [21] D. Tele, N. Wakhare, R. Bhosale, P. Bharde, S. Nerkar. Int. J. of Current Engineering and Technology, Special Issue-6 (2016) 74-77.
- [22] W.D. Callister, Jr. Materials Science and Engineering-An Introduction, John Wiley&Sons, 2007.
- [23] Multi-axial filament winding machine.<http://www.directindustry.com/prod/vem-spa/product-68234-505599.html>
- [24] Technical System Targets: Onboard Hydrogen Storage for Light-Duty Fuel Cell Vehicles
http://energy.gov/sites/prod/files/2015/01/f19/fcto_myrrdd_table_onboard_h2_storage_systems_doe_targets_ldv.pdf
- [25] S. Satyapal, S. Petrovic, G. Thomas, C. Read, G. Ordaz, “The U.S. national hydrogen storage project”, Proceedings The 16th World Hydrogen Energy Conference, 13-16 June, Lyon, France, 2006, pp. 1/10-9/10
- [26] G. Sandrock, J. Reilly, J. Graetz, W.-M. Zhou, J. Johnson, J. Wegrzyn, “Accelerated thermal decomposition of AlH_3 for hydrogen-fueled vehicles”, Appl. Phys. A 80 (2005) 687-690.
- [27] W. Grochala, P.P. Edwards, “Thermal decomposition of the non-interstitial hydrides for the storage and production of hydrogen”, Chemical Reviews 104 (2004) 1283-1315.
- [28] S-J. Hwang, R. C. Bowman, Jr., J. W. Reiter, J. Rijssenbeek, G. L. Soloveichik, Ji Cheng Zhao, Houria Kabbour,| C. C. Ahn. J. Phys. Chem, C Letters 112 (2008) 3164-3169.
- [29] J. Yang, A. Sudik, C. Wolverton, D.J. Siegel. Chem Soc. Rev. 39 (2010) 656-675.
- [30] L. H. Rude, T. K. Nielsen, D. B. Ravnsbæk, Ulrike Bösenberg, M. B. Ley, Bo Richter, L. M. Arnbjerg, M. Dornheim, Y. Filinchuk, F. Besenbacher, T. R. Jensen. Phys. Status Solidi 208 (2011) 1754–1773.
- [31] Eun Jeon, Young Whan Cho, “Mechanochemical synthesis and thermal decomposition of zinc borohydride”, J. Alloys Compd. 422 (2006) 273-275.
- [32] S. Srinivasan, E. Stefanakos, Y. Goswami, “New transition metal assisted complex borohydrides for hydrogen storage”, Proceedings The 16th World Hydrogen Energy Conference, 13-16 June, Lyon, France, 2006, pp. 1/6-6/6

- [33] A. Shirani Bidabadi, R.A. Varin, M. Polanski, L. Stobinski. RSC Adv. 6 (2016) 93245–93258.
- [34] R.A. Varin, D.K. Mattar, A. Shirani Bidabadi, M. Polanski. J. Energy Chemistry 26 (2017) 24-34.
- [35] R.A. Varin 1, D.K. Mattar, M. Polanski, A. Shirani Bidabadi, L. Stobinski. Energies 10 (2017) 1741.
- [36] R.A. Varin, A. Shirani Bidabadi, M. Polanski, M. Biglari, L. Stobinski. Mater. Res. Bull. 100 (2018) 394-406.
- [37] Hydrogen. https://en.wikipedia.org/wiki/Hydrogen#Discovery_and_use.
- [38] William Robert Grove. https://en.wikipedia.org/wiki/William_Robert_Grove.
- [39] T. Graham. Phil. Trans. Roy. Soc. (London), 156 (1866) 399-439.
- [40] A. Sieverts. Z. Phys. Chem. 60 (1907) 129-201.
- [41] A. Sieverts, G. Zapf, H. Moritz. Z. Phys. Chem. 183 (1938) 19-37.
- [42]. A. Sieverts, E. Jurish, A. Metz. Z. Anorg. Chem. 91 (1915) 1-45.
- [43] L. Kirschfeld, A. Sieverts. Z. Phys. Chem., 145(3-4) (1929) 227-240.
- [44] M. Avrami. J. Chem. Phys. 8 (1940) 212.
- [45] M. Avrami. J. Chem. Phys. 7 (1939) 1103.
- [46] M. Avrami. J. Chem. Phys. 9 (1941) 177.
- [47] G.G. Libowitz, H.F. Hayes, T.R.P. Gibb Jr. J. Phys. Chem. 62 (1958) 76.
- [48] B. Baranowski, M. Smialowski, J. Phys. Chem. Sol. 12 (1960) 206-207.
- [49] B. Barnowski, “Metal-hydrogen systems at high hydrogen pressures, in Hydrogen in Metals II”, G. Alefeld, J. Völkl, Editor. 1978, Springer-Verlag: Berlin-Heidelberg. pp. 157-200.
- [50] J.J.G. Willems, K.H.J. Buschow. J. Less-Comm. Metals, 129 (1987) 13-30.
- [51] H. Zijlstra, F.F Westendorp. Solid State Comm. 7 (1969) 857-859.
- [52] J.H.N. van Vucht, F.A. Kuijpers, H.C.A.M. Bruning. Philips Res. Repts. 25 (1970) 133-140.
- [53] J.J Reilly, R.H. Wiswall Jr., US Patent 3,825,418 “Alloys for the isolation of hydrogen”, 1974, Brookhaven National Laboratory: USA.
- [54] G.D. Sandroek, “Development of low cost nickel-rare Earth hydrides for hydrogen storage”, in Hydrogen Energy Systems, S.W. Veziroglu T.N., Editor. 1978, Pergamon Press. pp. 1625-1656.

- [55] Y. Osumi, H. Suzuki, A. Kato, M. Nakane, Y. Miyake. *J. Chem. Soc. Japan, Chem. and Industrial Chem.*, (Nippon Kagaku Kaishhi), No.11 (1978) 1472-1477.
- [56] H.H. van Mal, K.H.J. Buschow, F.A. Kuijpers. *J. Less-Common Metals*, 32 (1973) 289-296.
- [57] G.D. Sandrock, "A new family of hydrogen storage alloys based on the system nickel - mischmetal-calcium", in *Proc. 12th Intersociety Energy Conversion Engineering Conference*. Washington, D.C., USA, 28 August-2 Sept. 1977: Am. Nuclear Soc. (1977) pp. 951-958.
- [58] C.E. Lundin, F.E. Lynch, "Modification of hydriding properties of AB₅ alloy type hexagonal alloys through manganese substitution", in *Proc. of the Miami Int. Conf. Alternate Energy Sources*. United States, 5-7 Dec. 1977: University of Miami (1978) pp. 3803-3820.
- [59] M. Beltowska-Brzezinska, A. Czerwinski, J. Kleperis, M. Kopczyk, J. Skowronski, G. Wojcik. *J. Solid State Electrochem.*, 5 (2001) 229-249.
- [60] J.J. Reilly, R.H. Wiswall. *Inorg. Chem.*, 13 (1974) 218.
- [61] G. Sandrock. *J. Alloys&Compd.* 293-2958 (1999) 877-888.
- [62] C. Winkler. *Berichte der Deutwchen Chemischen Gasellschaft* 24 (1891) 1966.
- [63] F.H. Ellinger, C.E. Holley Jr., B.B. McInteer, D. Pavone, R.M. Potter, E. Staritzky, W.H. Zachariasen. *J. Am. Chem. Soc.*, 77 (1955) 2647.
- [64] E. Wiberg, H. Goeltzer, R. Bauer, *Z. Naturforsch, Teil B*, 6 (1951) 394; cited after B. Bogdanović, S-T. Liao, M. Schwickardi, P. Sikorsky, B. Spliethoff, "Catalytic synthesis of magnesium hydride under mild conditions", *Angew. Chem. Int. Ed. Engl.* 19 (1980) No.10, 818-819.
- [65] N.T. Dymova, Z.K. Sterlyadkina, V.G. Safranov, *Zh. Neorg. Khim. (J. Inorganic Chemistry)*, 6 (1961) 763; cited after B. Bogdanović, S-T. Liao, M. Schwickardi, P. Sikorsky, B. Spliethoff, "Catalytic synthesis of magnesium hydride under mild conditions", *Angew. Chem. Int. Ed. Engl.* 19 (1980) No.10, 818-819.
- [66] D.Z. Noreus. *Phys. Chem. NF*, 163 (1989) 575-578.
- [67] A. Pebler, E.A. Gulbransen. *Electrochem. Techn.* 4 (1966) 211-215.
- [68] J.J. Didishiem, P. Zolliker, K. Yvon, P. Fischer, J. Schefer, M. Grubelmann, A.F. Williams. *Inorg. Chem.*, 23 (1984) 1953-1957.
- [69] P. Selvam, K. Yvon. *Int. J. Hyd. Ener.*, 9 (1991) 615-617.
- [70] N.T. Stetson, K. Yvon, P. Fischer. *Inorg. Chem.* 33 (1994) 4598-4599.
- [71] B. Siegel. *J. Am. Chem. Soc.* 82 (1960) 7.

- [72] T.N. Dymova, N.G. Eliseeva, S.I. Bakum, Y.M. Dergachev. Dokl. Akad. Nauk SSSR, 215 (1974) 1369-1372.
- [73] B. Bogdanović, M. Schwickardi, "Ti-doped alkali metal aluminium hydrides as potential novel reversible hydrogen storage materials", J. Alloys Compd, 1-9 (1997) 253-254.
- [74] T.N. Dymova, Y.M. Dergachev, V.A. Sokolov, N.A. Grechanaya. Dokl. Nauk SSSR, 225 (1975) 591-592.
- [75] D. Goerrig, German Patent DE1077644. 1958: Germany.
- [76] V.N. Konoplev, V.M. Bakulina. Russian Chemical Bulletin (Translated from Izvestiya Akad.Nauk SSSR, Ser. Khim.), 20(1) (1971) 136-138.
- [77] A. Züttel, P. Wenger, S. Rentsch, P. Sudan. J. Power Sources, 118 (2003) 1-7.
- [78] M. Fichtner, G. Engel, O. Fuhr, A. Gloss, O. Rubner, R. Ahlrichs. Inorg. Chem. 42 (2003) 7060-7066.
- [79] <http://www.usetute.com.au/heatform.html>
- [80] <http://www.chem.tamu.edu/class/fyp/stone/tutorialnotefiles/thermo/enthalpy.htm>;
<http://www.chem.tamu.edu/class/fyp/stone/tutorialnotefiles/kinetics/activation.htm>.
- [81] D. Chandra D, J.J. Reilly, R. Chellappa. JOM 58 (2006) 26-32.
- [82] S. Qian, D.O. Northwood. Int. J. Hyd. Ener. 13 (1988) 25-35.
- [83] S. Qian, D.O. Northwood. Int. J. Hyd. Ener. 15 (1990) 649-654.
- [84] A.Y. Esayed, D.O. Northwood. Int. J. Hyd. Ener. 17 (1992) 41-52.
- [85] A. Andreasen, (2005) PhD thesis. Risø National Laboratory, Roskilde, Denmark.
- [86] R.B Schwarz. MRS Bulletin 24(11) (1999) 40-44.
- [87] H. Kissinger, Analytical Chem. "Reaction kinetics in differential thermal analysis", 29 (1957) 1702-1706.
- [88] N. Bazzanella, R. Checchetto, A. Miotello. Appl. Phys. Lettr. 85 (2004) 5212-5214.
- [89] K.F. Kelton. Mater. Sci. Eng. A 226-228 (1997) 142-150.
- [90] M.H. Mintz, Y. Zeiri. J. Alloys Compd. 216 (1994) 159-175.
- [91] T.R. Jensen, A. Andreasen, T. Vegge, J.W. Andreasen, K. Ståhl, A.S. Pedersen, M.M. Nielsen, A.M. Molenbroek, F. Besebbacher. Int. J. Hyd. Ener. 31 (2006) 2052-2062.
- [92] G. Barkhordarian, T. Klassen, R. Bormann. J. Alloys Compd. 364 (2004) 242-246.
- [93] G. Barkhordarian, T. Klassen, R. Bormann. J. Alloys Compd. 407 (2006) 249-255.
- [94] G. Liang, J. Huot, S. Boily, A. Van Neste, R. Schulz. J. Alloys Compd. 291 (1999) 295-299.

- [95] J. Huot, G. Liang, S. Boily, A. Van Neste, R. Schulz. *J. Alloys Compd.* 293-295 (1999) 495–500.
- [96] R.A. Varin, S. Li, Z. Wronski, O. Morozova, T. Khomenko. *J. Alloys and Compd.* 390 (2005) 282–296
- [97] E. Ivanov, I. Konstanchuk, A. Stepanov, V. Boldyrev, “Magnesium mechanical alloys for hydrogen storage”, *J. Less-Comm. Metals*, 131 (1987) 25-29.
- [98] L. Zaluski, A. Zaluska, J.O. Strom-Olsen. *J. Alloys Compd.* 253-254 (1997) 70-79.
- [99] H. Gleiter, “Nanocrystalline materials”, *Prog. Mater. Sci.* 33 (1989) 223-315.
- [100] Y. Gogotsi, ed., “Nanomaterials Handbook”, Taylor & Francis CRC Press, 2006, p. 800.
- [101] J.S. Benjamin. *Metall. Trans.* 1 (1970) 2943-2951.
- [102] C. Suryanarayana, “Mechanical alloying and milling”, *Prog. Mater. Sci.*, 46 (2001) 1-184.
- [103] R.A. Varin, S. Li, Z. Wronski, O. Morozova, T. Khomenko, “The effect of sequential and continuous high-energy impact mode on the mechano-chemical synthesis of nanostructured complex hydride Mg_2FeH_6 ”, *J. Alloys Compd.* 390 (2005) 282-296.
- [104] R.A. Varin, T. Czujko, “Overview of processing of nanocrystalline hydrogen storage intermetallics by mechanical alloying/milling”, *Mater. Manuf. Proc.* 17 (2002) 129-156.
- [105] R.A. Varin, Ch. Chiu, T. Czujko, Z. Wronski. *Nanotechnology* 16 (2005) 2261-2274.
- [106] J.M. Bellosta van Colbe, M. Felderhoff, B. Bogdanović, F. Schüth, C. Weidenthaler, *Chem. Commun.* (2005) 4732.
- [107] Z. Wronski, R.A. Varin, Ch. Chiu, T. Czujko, A. Calka, “Mechanochemical synthesis of nanostructured chemical hydrides in hydrogen alloying mills”, *J. Alloys and Compd.* 434-435 (2007) 743-746.
- [108] R.H. Perry, D.W. Green, J.O. Maloney, eds., “Perry's Chemical Engineers Handbook”, 50 ed. 1984, New York-Toronto: McGraw-Hill Book Company. p. 8-32.
- [109] R.W. Rydin, D. Maurice, T.H. Courtney. *Met. Trans. A*, 24A (1993) 175-185.
- [110] D.R. Maurice, T.H. Courtney, “The physics of mechanical alloying: A first report”, *Met. Trans. A*, 21 (1990) 289-303.
- [111] S.N. Zhurov, “Mechanochemistry: The mechanical activation of covalent bonds”, *Inter. J. Fracture Mechanics*, 1 (1965) 311.
- [112] R.A. Varin, T. Czujko, Z.S. Wronski. *J. Alloys Compd.* 17 (2006) 3856-3865.

[113] Policy Statement on Health Canada's Working Definition for Nanomaterial" available in English at: <http://www.hc-sc.gc.ca/sr-sr/pubs/nano/pol-fra.php>.

[114] H.-J. Fecht. NanoStructured Materials. 6 (1995) 33-42.

[115] H.P. Klug and L. Alexander, "X-ray Diffraction Procedures for Polycrystalline and Amorphous Materials", John Wiley & Sons, New York (1st Ed. 1954, 2nd Ed. 1974).